



ARL-TR-9649 • FEB 2023



Randomized Linear Receive Arrays for Through-the-Wall Moving Target Indication

by Kenneth Ranney, Anthony Martone, and Roberto Innocenti

Approved for public release: distribution unlimited.

NOTICES

Disclaimers

The findings in this report are not to be construed as an official Department of the Army position unless so designated by other authorized documents.

Citation of manufacturer's or trade names does not constitute an official endorsement or approval of the use thereof.

Destroy this report when it is no longer needed. Do not return it to the originator.



Randomized Linear Receive Arrays for Through-the-Wall Moving Target Indication

Kenneth Ranney, Anthony Martone, and Roberto Innocenti
DEVCOM Army Research Laboratory

REPORT DOCUMENTATION PAGE

1. REPORT DATE		2. REPORT TYPE		3. DATES COVERED	
February 2023		Technical Report		START DATE	END DATE
				1/11/2011	12/31/2011
4. TITLE AND SUBTITLE					
Randomized Linear Receive Arrays for Through-the-Wall Moving Target Indication					
5a. CONTRACT NUMBER		5b. GRANT NUMBER		5c. PROGRAM ELEMENT NUMBER	
5d. PROJECT NUMBER		5e. TASK NUMBER		5f. WORK UNIT NUMBER	
6. AUTHOR(S)					
Kenneth Ranney, Anthony Martone, and Roberto Innocenti					
7. PERFORMING ORGANIZATION NAME(S) AND ADDRESS(ES)				8. PERFORMING ORGANIZATION REPORT NUMBER	
DEVCOM Army Research Laboratory ATTN: FCDD-RLA-LC Adelphi, MD 20783				ARL-TR-9649	
9. SPONSORING/MONITORING AGENCY NAME(S) AND ADDRESS(ES)			10. SPONSOR/MONITOR'S ACRONYM(S)	11. SPONSOR/MONITOR'S REPORT NUMBER(S)	
12. DISTRIBUTION/AVAILABILITY STATEMENT					
Approved for public release: distribution unlimited.					
13. SUPPLEMENTARY NOTES					
ORCID ID: 0000-0002-1283-6206, Kenneth Ranney					
14. ABSTRACT					
Azimuthal sidelobe reduction remains a significant challenge in many current radar applications, including detection of slowly moving targets inside buildings. We consider a linear receive array and introduce a sidelobe-reduction technique that operates in the time domain to reduce artifacts in output imagery produced by a near-field beam-sharpener. We then demonstrate the effectiveness of this technique using data collected by an impulse-based, low-frequency, ultra-wideband radar used for through-the-wall, moving-target indication (MTI) at near-range. We implement a change detection paradigm for MTI, since this approach is most appropriate for the radar system under consideration. Finally, we introduce metrics to quantify the improvements in MTI image quality realized through the introduction of randomized linear arrays.					
15. SUBJECT TERMS					
Electromagnetic Spectrum Sciences, moving-target indication, recursive sidelobe minimization, apodization, sidelobe reduction, ultra-wideband radar, sensing-through-the-wall radar, low-frequency radar					
16. SECURITY CLASSIFICATION OF:			17. LIMITATION OF ABSTRACT		18. NUMBER OF PAGES
a. REPORT	b. ABSTRACT	c. THIS PAGE	UU		15
UNCLASSIFIED	UNCLASSIFIED	UNCLASSIFIED			
19a. NAME OF RESPONSIBLE PERSON				19b. PHONE NUMBER (Include area code)	
Kenneth Ranney				(301) 394-0832	

STANDARD FORM 298 (REV. 5/2020)

Prescribed by ANSI Std. Z39.18

Contents

List of Figures	iv
1. Introduction	1
2. MTI Image Formation	2
3. Randomized Linear Array (RLA) Processing	3
4. RLA-Generated CD Imagery	4
5. Summary and Conclusion	6
6. References	7
List of Symbols, Abbreviations, and Acronyms	8
Distribution List	9

List of Figures

Fig. 1	Example of CD image showing a man walking behind a cinderblock wall. The dynamic range of the image is 30 dB (relative to the peak pixel value). The image begins at 8 m (in downrange) from the radar.	3
Fig. 2	Representation of the imaging geometry for the RLA experiments. The walls are cinderblock, and the SIRE system includes 16 receive channels. The two transmitters are located at either end of the receive array.	5
Fig. 3	Examples of CD imagery produced by RLA algorithm. Note the absence of the sidelobe “arcs” evident in Fig. 1. The dynamic range of the image is 30 dB (relative to the peak pixel value)—the same color scale as Fig. 1.	5
Fig. 4	Example of CD image showing a man walking behind a cinderblock wall. The dynamic range of the image is 30 dB (relative to the peak pixel value)—the same color scale as Fig. 1.	6
Fig. 5	Image showing reduction in sidelobe level (in dB) realized by the RLA processing	6

1. Introduction

Detection of targets hidden behind walls remains an important area of research within the radar community, and many researchers have recently reported interesting findings.¹⁻⁵ The need for effective wall penetration has often driven investigators to consider systems utilizing lower frequencies, while the need for high resolution has driven them to consider large-bandwidth systems. One such system—the US Army Combat Capabilities Development Command (DEVCOM) Army Research Laboratory’s (ARL’s) ultra-wideband (UWB) synchronous impulse reconstruction (SIRE) radar—includes both of these characteristics. Not surprisingly, it has shown promise when leveraged for sensing-through-the-wall (STTW) applications.^{4,6}

Much of our past moving-target indication (MTI) work centered on STTW detection of moving targets using SIRE radar data.^{4,5} This work, however, has not incorporated newly formulated extensions of documented synthetic aperture radar (SAR) techniques,⁷ and inclusion of these adapted techniques should produce higher quality MTI imagery. In particular, they should eliminate artifacts in cross range due to time-domain focusing methodologies such as time-domain back-projection.

In this report, we introduce an artifact-reduction technique for near-field, time-domain, through-the-wall (TTW) MTI image-formation algorithms. The technique exploits measurements from multiple realizations of a randomly configured, linear receive array, rather than simply processing measurements from the original array. This “multi-array” processing effectively reduces cross-range sidelobe artifacts at the expense of additional computational complexity. We implement the randomly configured, linear receive arrays through the random excision of a subset of available receive channels, and we then produce the output MTI image through a judicious combination of imagery created with the various sub-arrays. Components of the procedure are presented in detail.

Section 2 describes the MTI image formation procedure and system-related issues that led to the implementation of this approach. Section 3 describes the randomized linear array (RLA) processing scheme in detail, noting some potential problems to be avoided in implementing the algorithm. Section 4 presents results obtained using MTI data collected by the SIRE radar system and processed using the RLA algorithm. A comparison of these results to those obtained using the standard linear array processing is also presented.

2. MTI Image Formation

Classical narrowband MTI systems often operate in the range-Doppler domain under the assumption that targets are located kilometers from the radar platform. This assumption allows wave fronts at the receive array to be considered planar and enables beam-steering to be performed via a linear phase adjustment across the array. Since the SIRE radar operates at close range, however, this plane-wave assumption is no longer valid. In addition, the SIRE system’s unique processing architecture makes it particularly well-suited to time-domain rather than Doppler-domain processing. These system attributes, combined with the low velocity of the targets to be prosecuted, led us to implement an MTI approach based on a change detection (CD) paradigm.^{4,5} The resulting time-domain approach has proven to be extremely effective for detecting slowly moving targets as part of the STTW application.

As an initial MTI processing step, we use a time-domain, back-projection algorithm to focus energy within the scene⁸ using one *frame* of data, where a *frame* comprises measurements from the pairwise combination of transmit and receive channels for a single sequence of transmit pulses. We recall here that 1) the SIRE system includes 2 transmit and 16 receive channels and 2) the transmitters fire in an alternating sequence. Thus, each frame of data contains 32 measurements at each available downrange location. The back-projection algorithm combines all of this information to produce an output image for each frame, and pairs of images from adjacent frames are then coherently subtracted to produce the final MTI image as summarized by

$$I_k(x, y) = \sum_{i=1}^{16} \sum_{j=1}^2 g(r_{i,j}) f_{i,j,k}(r_{i,j}) \quad (1)$$

and

$$\Delta_k(x, y) = I_{k+1}(x, y) - I_k(x, y), \quad (2)$$

where $r_{i,j}$ represents the range gate corresponding to the transmitter/receiver pair (j , i) and image pixel (x,y) , $g(r_{i,j})$ represents a weighting function, $f_{i,j,k}(r_{i,j})$ represents the raw data from transmitter j , receiver i , and time index k at range gate $r_{i,j}$, $I_k(x,y)$ represents the image pixel at coordinate (x,y) at time index k , and Δ_k is the CD image at time index k used for MTI processing.

Although the subtraction step in Eq. 2 suppresses much of the background clutter, certain MTI imaging artifacts still remain, as evidenced by Fig. 1. The scenario for this data collection comprised a lone man walking in a structure with cinderblock walls. The necessary data were collected by the stationary SIRE radar and then filtered to the 500–1500 MHz frequency band prior to image formation. The

sidelobes associated with various objects are clearly visible in Fig. 1. We will mitigate these effects via the introduction of randomized linear array processing.

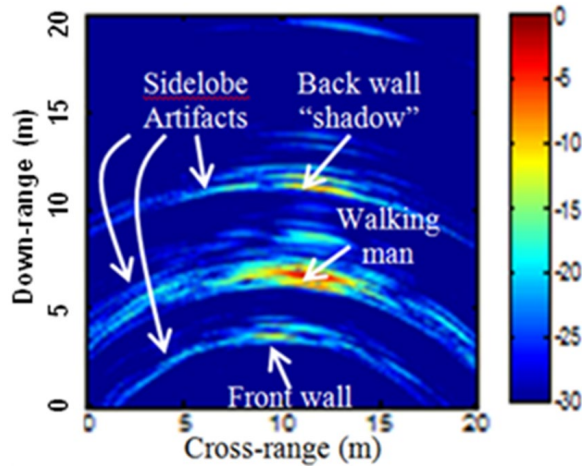


Fig. 1 Example of CD image showing a man walking behind a cinderblock wall. The dynamic range of the image is 30 dB (relative to the peak pixel value). The image begins at 8 m (in downrange) from the radar.

3. Randomized Linear Array (RLA) Processing

Randomized array processing is, at its core, an adaptation and extension of the recursive sidelobe minimization (RSM) algorithm developed for synthetic aperture radar (SAR).^{7,9} There is, however, a difference in implementation. While the earlier RSM algorithm required a moving platform and 2-D synthetic aperture as part of its image formation and sidelobe reduction procedures, we require only the 1-D aperture afforded by the linear receive array. This is due to the high degree of clutter cancellation achieved through MTI CD processing, which effectively eliminates the background clutter returns competing with both targets and sidelobe artifacts. If the clutter cancellation were not available, then the RLA algorithm would not be practicable.

We begin our description of the RLA algorithm by noting that it is an iterative process. During each iteration of the RLA algorithm, we remove a different, randomly selected subset of receive channels from the complete set available for MTI image formation. After the algorithm completes its first iteration, the complex magnitude of the newly created CD image (i.e., the *magnitude image*) is saved. This magnitude image then becomes our output CD image. During subsequent iterations we compare each pixel of the current CD image with the corresponding pixel of the output CD image. If the current magnitude is smaller than the output magnitude, then we replace the output value with the current one. We repeat this procedure until either a predetermined number of iterations have been performed or no further changes in output pixel values are observed.

The procedure is summarized as follows for a fixed number of iterations:

- 1) Determine the number of iterations, N , and initialize the output image variable, O , to an array of zeros.
- 2) Randomly generate N sets of M indices to be excised from the L transmit/receive pairs.
- 3) Form N coherent-difference CD images using the N sets of $(L - M)$ indices selected in step 2.
- 4) Calculate the output image according to

$$O(x, y) = \min_k \{|\Delta_k(x, y)|\} \quad (3)$$

where $1 \leq m \leq N$ corresponds to a particular set of deleted transmit/receive pairs and $\Delta_k(x, y)$ is defined in Eq. 2.

Since the sidelobe pattern in $\Delta_k(x, y)$ varies from one realization to the next, the operation in Eq. 3 suppresses the overall sidelobe response. The target (mainlobe) response, however, remains consistent for all realizations (see Eqs. 1 and 2); hence, it is not attenuated. From these observations it becomes clear that the minimum in Eq. 3 is the mechanism whereby the RLA algorithm can produce higher-quality CD imagery.

Note that the same set of random indices must be used for each constituent image of the CD difference (i.e., $I_k(x, y)$ and $I_{k+1}(x, y)$). The use of different indices would result in different sidelobe patterns, and the output CD image would be destroyed.

4. RLA-Generated CD Imagery

The effectiveness of the proposed RLA approach is illustrated in Fig. 2. To generate this image, we set $N = 100$, and $M = 5$ in step 3, and we used data from the same SIRE radar data collection used to generate the CD image in Fig. 1. Recall that in this scenario the test subject walked randomly inside a structure with cinderblock walls while the stationary SIRE radar collected data with the axis of its receive array parallel to the front wall of the building. The data collection configuration is illustrated in the diagram in Fig. 2. More specific details regarding the experiment are provided in Martone et al.⁵

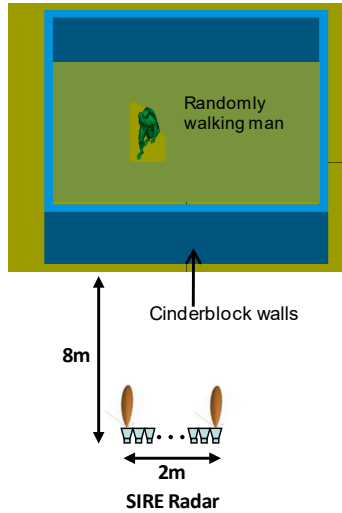


Fig. 2 Representation of the imaging geometry for the RLA experiments. The walls are cinderblock, and the SIRE system includes 16 receive channels. The two transmitters are located at either end of the receive array.

In Fig. 3, we immediately see that the sidelobe “arcs” present in Fig. 1 are largely eliminated. This observation is confirmed by the imagery in Fig. 4, which shows the non-RLA images corresponding to the RLA images in Fig. 3. The color scales and data collection geometry used to generate this imagery are the same as that used to generate the imagery in Fig. 1.

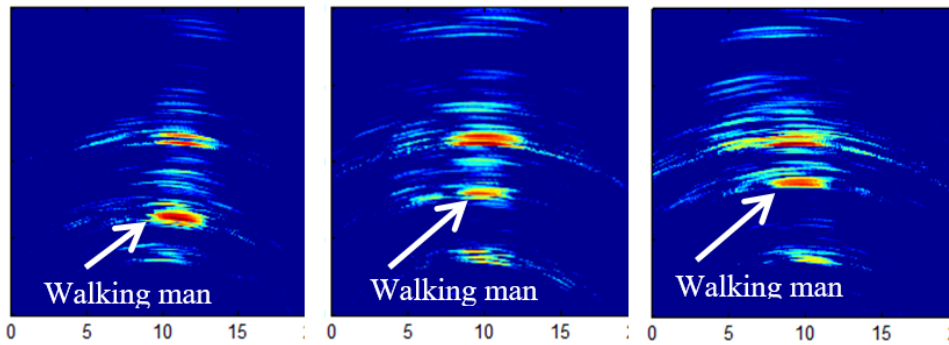


Fig. 3 Examples of CD imagery produced by RLA algorithm. Note the absence of the sidelobe “arcs” evident in Fig. 1. The dynamic range of the image is 30 dB (relative to the peak pixel value)—the same color scale as Fig. 1.

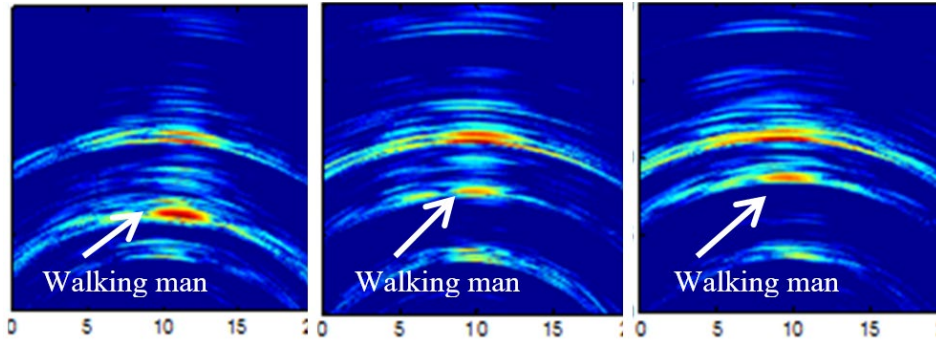


Fig. 4 Example of CD image showing a man walking behind a cinderblock wall. The dynamic range of the image is 30 dB (relative to the peak pixel value)—the same color scale as Fig. 1.

We have also calculated the relative reduction in sidelobe level (in dB) obtained using the RLA processing; the results are shown in Fig. 5 for the previously considered test images, where the peak image value is set to 0 dB. In order to better visualize these results, we selected a floor of -15 dB and set all pixels in the image below -15 dB to -15 dB. From the images in Fig. 5, we see that a reduction in sidelobe level of more than 15 dB is possible. Such reductions should translate readily to a reduction in false alarms.

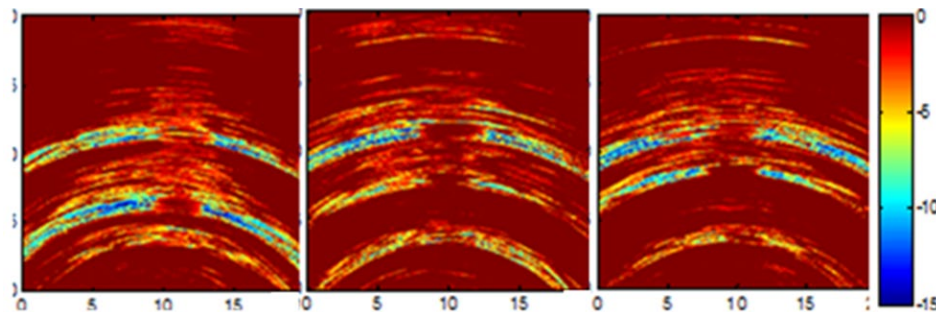


Fig. 5 Image showing reduction in sidelobe level (in dB) realized by the RLA processing

5. Summary and Conclusion

We described a procedure for reducing the number and severity of artifacts in MTI imagery. In particular, we discussed how this RLA algorithm can effectively eliminate many of the sidelobes produced by objects within an area under surveillance. We documented the effectiveness of the new technique, leveraging available STTW data collected with ARL’s low-frequency UWB SIRE radar system. Results indicated that, at certain MTI image pixels, a reduction in sidelobe level of more than 15 dB can be realized. Such reductions could translate readily to a reduction in false alarms. Higher quality input MTI imagery could only aid downstream processing.

6. References

1. Farwell M, Ross J, Luttrell R, Cohen D, Chin W, Dogaru T. Sense through the wall system development and design considerations. *J Franklin Inst.* 2008 Sep;345(6):570–591.
2. Amin M, Ahmad F, Zhang W. Target RCS exploitations in compressive sensing for through wall imaging. *Proceedings of the 2010 International Waveform Diversity and Design Conference*; 2010 Aug; Niagara Falls, ON, Canada.
3. Setlur P, Ahmad F, Smith G, Amin M. Multipath analyses of moving targets in enclosed structures using Doppler radars. *Proceedings of SPIE.* 2010;7669.
4. Martone A, Ranney K, Innocenti R. Automatic through the wall detection of moving targets using low-frequency ultra-wideband radar. *Proceedings of the IEEE International radar conference*; 2010 May; Washington, DC.
5. Martone A, Ranney K, Innocenti R. Through-the-wall detection of slow-moving personnel. *Proceedings of SPIE.* 2009;7308.
6. Le C, Dogaru T, Nguyen L, Ressler MA. Ultrawideband (UWB) radar imaging of building interior: measurements and predictions. *IEEE Trans Geosci Remote Sens.* 2015;47(3):409–1420.
7. Nguyen L. SAR imaging technique for reduction of sidelobes and noise. *Proceedings of SPIE.* 2009;7308.\
8. McCorkle J. Focusing of synthetic aperture ultra wideband data. *Proceedings of the IEEE International Conference on Systems Engineering*; 1991 Aug; Dayton, OH. p. 1–5.
9. Martone AF, Ranney K, Le C. Noncoherent approach for through-the-wall moving target indication. In: *IEEE Transactions on Aerospace and Electronic Systems*, vol. 50, no. 1; 2014 Jan. p. 193–206.

List of Symbols, Abbreviations, and Acronyms

1-D	one-dimensional
2-D	two-dimensional
ARL	Army Research Laboratory
CD	change detection
DEVCOM	US Army Combat Capabilities Development Command
MTI	moving-target indication
RLA	randomized linear array
RSM	recursive sidelobe minimization
SAR	synthetic aperture radar
SIRE	synchronous impulse reconstruction
STTW	sensing through the wall
TTW	through the wall
UWB	ultra-wideband

1 DEFENSE TECHNICAL
(PDF) INFORMATION CTR
DTIC OCA

1 DEVCOM ARL
(PDF) FCDD RLB CI
TECH LIB

2 DEVCOM ARL
(PDF) FCDD RLA LC
K RANNEY
A MARTONE